Hydrogenation of semiconductor surfaces: Si-terminated cubic SiC(100) surfaces

Daniel G. Trabada, Fernando Flores, and José Ortega
Departamento de Física Teórica de la Materia Condensada, Universidad Autónoma de Madrid, E-28049 Madrid, Spain
(Received 28 April 2009; revised manuscript received 29 June 2009; published 13 August 2009)

We analyze the hydrogenation of the Si-terminated surfaces 3C-SiC(100)-3×2 and 3C-SiC(100)-$c(4\times2)$ using density-functional-theory techniques. For the Si-rich 3×2 case, after saturation of the Si dangling bonds, hydrogen atoms break Si-Si bonds between atoms in the first two layers, replacing them by Si-H bonds, up to a hydrogen adsorption of eight hydrogen atoms per 3×2 unit cell, with the formation of SiH_3 groups on the surface. At higher hydrogen adsorptions Si-H bonds replace also Si-Si bonds between second- and third-layer Si atoms. We find that all the stable structures as a function of the hydrogen chemical potential are insulating and propose that the observed hydrogen-induced metallization of the Si-rich SiC(100)-3×2 surface is related to the dynamical equilibrium between adsorption and abstraction of hydrogen atoms close to the point where hydrogen atoms start to break Si-Si bonds. We also find that desorption of SiH_4 molecules is not energetically favorable until values of the hydrogen chemical potential above half the energy of the H_2 molecule. Regarding the Si-poor $c(4\times2)$ surface, our results show that the hydrogenated H/SiC(100)-2×1 surface corresponds to a monohydride surface with a Si coverage of one monolayer above the last C layer.

DOI: 10.1103/PhysRevB.80.075307 PACS number(s): 68.43.Bc

I. INTRODUCTION

The hydrogenation of semiconductor surfaces is a topic of great interest,[1–10] The interaction of hydrogen with semiconductor surfaces generally induces important structural and electronic changes. In general, adsorption of hydrogen produces passivation of the surface; the hydrogen atoms attach to the semiconductor dangling bonds, forming strong chemical bonds (chemical passivation) and removing electronic states from the semiconductor gap (electronic passivation). In addition to saturating the semiconductor dangling bonds, hydrogen atoms can also be located below the last semiconductor atomic layer, changing the electrical conductivity of the surface.

The interaction of hydrogen with semiconductor surfaces has been intensively investigated,[1–10] specially for silicon surfaces. There are several reasons for this interest. From a fundamental point of view, the interaction of hydrogen with silicon surfaces has been used as a model system to study chemisorption on semiconductor surfaces. Also, the interaction of hydrogen with semiconductor surfaces has been used to investigate the atomic structure of clean semiconductor surfaces. From an applied perspective, hydrogenation of semiconductor surfaces is of central importance in semiconductor technologies.

Silicon Carbide (SiC) is a wideband-gap semiconductor with interesting properties for high-temperature, high-power, and high-frequency applications in electronics.[5,11–13] SiC crystals exist in diverse stacking arrangements of the atomic planes such as hexagonal 6H and 4H and cubic 3C polytypes. Recently, SiC surfaces have attracted a lot of attention[14–21] due to their remarkable physical properties, which include a temperature-induced reversible structural and metal-insulator transition,[14] Mott-insulating surfaces,[15,16] self-organized one-dimensional Si chains,[17] and even a surprising hydrogen-induced metallization of a semiconductor surface.[18] Of special interest are the (100) surfaces of cubic SiC with Si termination, 3C-SiC(100)-3×2 and 3C-SiC(100)-$c(4\times2)$.[11–13] SiC(100)-3×2 is the Si-saturated 3C-SiC(100) surface. The atomic structure of this surface seems to be well established.[12,13,22] As shown in Fig. 1(a), SiC(100)-3×2 presents three Si layers on top of the last C layer, with a total Si coverage of two monolayers (ML), $\theta=2$. Regarding the atomic structure of the Si-poor 3C-SiC(100)-$c(4\times2)$ there is some controversy[12,13,23] whether this surface corresponds to a Si coverage of $\theta=1$ (Ref. 24) or $\theta=1.5$.[25] At the transition between the Si-rich SiC(100)-3×2 and Si-poor SiC(100)-$c(4\times2)$ selective thermal removal of Si atoms results in self-organized Si atomic lines.[17,26]

The hydrogenation of the 3C-SiC(100)-3×2 surface has been analyzed experimentally by exposing a clean 3×2 surface to an atmosphere of H_2 molecules that includes atomic hydrogen dissociated by a hot tungsten filament. If the surface is kept at room temperature during hydrogen adsorption, this results in a passivated H/SiC(100)-3×1 surface at exposures of the order of 400–500 L (L=Langmuir).[27] At higher exposures the 3×1 order is destroyed and a 1×1 pattern is observed. On the other hand, if atomic exposures are performed keeping the surface at a temperature of 300 °C, metallization of the surface is observed for H_2 exposures of ~20 L.[18] This surprising result has prompted many studies on the hydrogenation of the 3C-SiC(100)-3×2 surface[18,28–39] but in spite of this effort the origin of this hydrogen-induced metallization, as well as the atomic structure of the H/SiC(100)-3×1 and H/SiC(100)-1×1 phases, remain a mystery.

While the 3C-SiC(100)-3×2 surface is inert upon interaction with molecular H_2, the SiC(100)-$c(4\times2)$ surface is highly reactive, with H_2 dissociation.[38,40] In this case, the surface changes to a 2×1 symmetry upon adsorption of hydrogen.

This transition is reversible since thermal desorption of hydrogen restores the original $c(4\times2)$ reconstruction.[40,41] Similarly, the 3C-SiC(100)-3×2 surface is recovered upon desorption of H at 900–1000 °C from either the Si-rich H/SiC(100)-3×1 or H/SiC(100)-1×1 surfaces.[27]

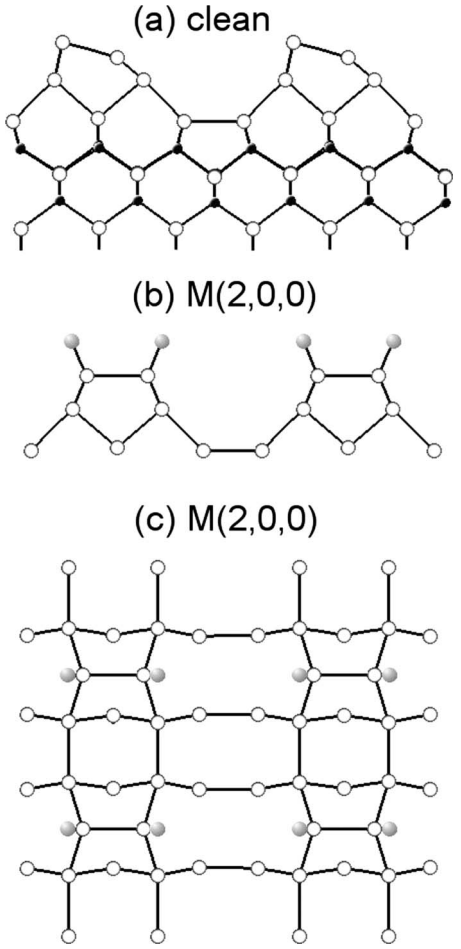

FIG. 1. Atomic models for (a) SiC(100)-3×2 clean surface and [(b) and (c)] the monohydride M(2,0,0) structure with hydrogen atoms saturating the Si dangling bonds. Open circles denote Si atoms, black circles C atoms, and gray circles H atoms. [(a) and (b)] Side views; (c) top view.

In this work we analyze the hydrogenation of the SiC(100)-3×2 and SiC(100)-$c(4\times2)$ surfaces using a combination of density-functional-theory (DFT) techniques.[42,43] For the Si-rich SiC(100)-3×2 surface, hydrogen atoms first saturate the semiconductor dangling bonds. In a second step, Si-Si bonds between Si atoms in the first two layers are replaced by Si-H bonds up to an adsorption of eight hydrogen atoms per 3×2 unit cell. At higher hydrogen adsorptions, Si-H bonds also replace Si-Si bonds between Si atoms in the second and third Si layers. We find that the formation of SiH_3 groups in the surface is energetically favorable for six or more hydrogen atoms in the 3×2 unit cell. The H/SiC(100)-3×1 and H/SiC(100)-1×1 phases are explained as resulting from the structural disorder along the $\times2$ and $\times3$ directions associated with the rupture of the Si-Si bonds between Si atoms in the first and second layers or the second and third Si layers, respectively. We find that all the stable structures as a function of the hydrogen chemical potential are insulating. Our results suggest that the observed hydrogen-induced metallization is associated with the equilibrium between adsorption and abstraction of hydrogen, when the surface is exposed to an atmosphere of atomic hydrogen, close to the point where incoming hydrogen atoms start to replace Si-Si bonds by Si-H bonds. We also analyze the desorption of SiH_4 molecules from the hydrogenated Si-rich surfaces and find that it is not energetically favorable until values of the hydrogen chemical potential higher than half the energy of the H_2 molecule. In the case of the Si-poor 3C-SiC(100)-$c(4\times2)$ surface, we find that for both Si coverages $\theta=1$ and $\theta=1.5$ the monohydride surfaces are the stable structures for all the values of interest for the hydrogen chemical potential. By comparing with the experimental evidence, we conclude that the hydrogenated Si-poor 2×1 surface presents a Si coverage of $\theta=1$.

II. THEORETICAL AND COMPUTATIONAL METHODS

We have studied the interaction of hydrogen with the Si-rich SiC(100)-3×2 and Si-poor SiC(100)-$c(4\times2)$ surfaces using two complementary DFT techniques. First, we explore many different atomic configurations, using an efficient molecular-dynamics DFT code [FIREBALL (Ref. 42)]. The most interesting relaxed structures are then further considered using the more accurate (but much more computationally intensive) plane-wave (PW) approach [CASTEP (Ref. 43)]. In this way we have analyzed more than 430 structures, with different hydrogen coverages using FIREBALL. Out of these structures, we selected 110 structures that were then further refined using the PW code.

For the FIREBALL calculations we have used an optimized $sp3$ basis of numerical atomiclike orbitals[44] for SiC and a double ss^* basis for hydrogen. For the PW calculations we use ultrasoft pseudopotentials and a PW cutoff energy of 280 eV. In both codes we have used the local-density approximation (LDA) exchange-correlation functional.[45] Calculations were also performed using the generalized gradient approximation (GGA) functional[46] for some key structures. In our calculations the 3C-SiC(100) surface is modeled by means of eight SiC layers and H atoms saturating the lowest C layer; the lowest two SiC layers are fixed at bulk positions. We have used a 3×2 or a 4×2 surface unit cells, for the SiC(100)-3×2 and SiC(100)-$c(4\times2)$ surfaces, respectively. In both cases, the surface Brillouin zone was sampled using eight special k points. For the Si-rich SiC(100)-3×2 case, two additional layers of Si atoms are added on top of the last full Si ML [see Fig. 1(a)] with two and four Si atoms per 3×2 unit cell in the first and second layers, respectively.

In order to analyze the relative stability of surface structures with different number of hydrogen atoms, we use the grand-canonical potential and calculate the adsorption energy E_a as a function of the hydrogen chemical potential μ_H (Refs. 31, 33, and 47)

$$E_a(\mu_H) = E[\mathrm{H/SiC(100)}] - E_{SURF} - N_H\mu_H, \qquad (1)$$

where N_H is the number of hydrogen atoms in the surface unit cell, $E[\mathrm{H/SiC(100)}]$ is the total energy for the hydrogenated surface under consideration, and E_{SURF} is the energy of the corresponding SiC(100)-3×2 or SiC(100)-4×2 clean surface. Due to the small mass of the hydrogen atoms, the zero-point energy associated with Si-H vibrations is also included in $E[\mathrm{H/SiC(100)}]$ by adding 0.21 eV per hydrogen

atom.[47] It is also useful to define an adsorption energy E_a^0, taking as reference the energy of the H_2 molecule

$$E_a^0 = E[\mathrm{H/SiC(100)}] - E_{\mathrm{SURF}} - \frac{N_{\mathrm{H}}}{2}E[\mathrm{H_2}], \qquad (2)$$

where $E[H_2]$ is the energy of the H_2 molecule (also including zero-point energy). In our LDA GGA PW calculations $E[H_2]=-30.88(-31.74)+0.27=-30.61(-31.47)$ eV (0.27 eV is the zero-point energy for H_2 molecule[47]). A negative value for E_a^0 indicates that H adsorption is favored over the H_2 gas phase. Equation (2) is a particular case of Eq. (1), that corresponds to taking the reference value $\mu_{\mathrm{H}}^0=\frac{1}{2}E[H_2]$ for the hydrogen chemical potential. Notice that μ_{H}^0 corresponds to the upper limit of the hydrogen chemical potential for a surface interacting with an atmosphere of H_2 molecules. Unless otherwise indicated, the results presented below correspond to the PW LDA calculations.

III. RESULTS AND DISCUSSION

A. Hydrogenation of the Si-rich SiC(100) surface

In the SiC(100)-3×2 surface there are three Si layers on top of the last C layer, with a total coverage of two Si ML, see Fig. 1(a). The upper layer consists of asymmetric Si dimers (1/3 Si ML) that are bonded on top of a second layer of Si dimers (2/3 ML). The third layer is a full ML of Si atoms that also contains Si dimers in order to fully passivate the surface.[22,26]

In this work we label the different H/SiC(100)-3×2 surface structures as $X(l,m,n)$, where l,m,n are the number of H atoms bonded to Si atoms in the first, second, and third layers, respectively; a letter X=M, D, T or B is included to further discriminate between similar H/SiC(100)-3×2 surface structures; T indicates that the structure presents one or more Si atoms bonded to three hydrogen atoms (i.e., a SiH_3 group or trihydride Si atom); D is used for structures with one or more SiH_2 groups (a Si atom bonded to two hydrogen atoms or dihydride Si atom), and no SiH_3 groups; M corresponds to structures with only monohydride Si atoms (SiH); finally, B is used to indicate that there are H atoms in bridge positions.

In the SiC(100)-3×2 surface there are two dangling bonds per 3×2 unit cell, that are located on the Si dimers of the top layer. On the clean surface the dimer is asymmetric, the dangling bond of the upper Si atom being fully occupied while the dangling bond of the lower Si atom is empty, thus the surface is semiconducting. When hydrogen atoms are deposited on this surface, they first bond to these dangling bonds, forming strong Si-H bonds. When all dangling bonds are saturated, we obtain structure M(2,0,0), see Figs. 1(b) and 1(c). The calculated adsorption energy for the M(2,0,0) structure, using Eq. (2), is $E_a^0=-1.97$ eV, showing the strong tendency of hydrogen atoms to saturate the semiconductor dangling bonds. As shown in Fig. 1(b), the Si dimers become symmetric upon adsorption of hydrogen atoms.

While there is general agreement that the first hydrogen atoms attach to the Si atoms of the first layer, saturating the dangling bonds with one hydrogen atom per Si atom (i.e., in a monohydride configuration), the interesting question is how subsequent hydrogen atoms react with this already well-passivated surface. Now, hydrogen atoms have basically two possibilities: either break a Si-Si bond or to attach to the surface in "bridge" positions, without breaking Si-Si bonds (in this work we have not considered the rupture of Si-C bonds). In agreement with other calculations[31,33] we find that energetically is clearly more favorable to break Si-Si bonds and replace them by Si-H bonds. In the SiC(100)-3×2 surface, starting from the M(2,0,0) structure, hydrogen atoms may replace different Si-Si bonds by Si-H bonds, such as the first-layer dimer bond, the bond between first- and second-layer Si atoms, bonds involving third-layer Si atoms, etc. As can be seen from Table I and Figs. 2 and 4 it is more favorable to first break the first-layer dimer bond and/or Si-Si bonds between first- and second-layer Si atoms; the rupture of Si-Si bonds involving third-layer Si atoms does not result in stable structures until a coverage of ten hydrogen atoms per 3×2 unit cell (see Fig. 5). Also, it is clear form Table I that structures involving an odd number of hydrogen atoms (per 3×2 unit cell), are markedly higher in energy as compared to structures with an even number of hydrogen atoms. Moreover, all the most stable structures (with an even number of hydrogen atoms) are insulating; saturation of dangling bonds by hydrogen atoms plus replacement of Si-Si bonds by pairs of Si-H bonds yield insulating structures.

Figures 2(a)–2(c) shows the most stable structures we have obtained for the adsorption of four hydrogen atoms per 3×2 unit cell. The most stable one (in agreement with previous calculations[31,33]) is the D(400) structure, Fig. 2(a), resulting from the rupture of the first-layer dimer bond with the formation of two SiH_2 units per 3×2 unit cell in the first Si layer. Close in energy (~0.1 eV) is structure D(310), that results from the rupture of a bond between first- and second-layer Si atoms, see Fig. 2(b). In this structure the first-layer Si-dimer bond is preserved and one SiH_2 unit is formed in the first layer. Figure 2(c) shows the best structure with only monohydride Si atoms M(2,1,1) (this structure is 0.04 eV lower than a similar M(2,1,1) structure found previously[33]).

Figures 2(d)–2(f) show the most stable structures we have obtained for the adsorption of six hydrogen atoms per 3×2 unit cell. These three structures involve the breaking of two Si-Si bonds: two different bonds between first- and second-layer Si atoms for structures T(4,2,0), Fig. 2(d), and D(4,2,0), Fig. 2(f), or the first-layer dimer bond plus a bond between first- and second-layer Si atoms in structure T(5,1,0), Fig. 2(e). These three structures present very similar total energies (see Table I), the most stable one being T(4,2,0). Notice that structures T(4,2,0) and T(5,1,0) already contain SiH_3 groups. These structures, as well as the most stable structures we have found for higher coverages $N_{\mathrm{H}} \geq 6$ (see Table I and Figs. 3–5) have not been considered in previous DFT calculations.[31,33,39] For example, our most stable structures for $N_{\mathrm{H}}=6$, 8, and 10 [T(4,2,0), T(6,2,0), and T(4,5,1)] are 0.44, 0.69, and 1.95 eV, respectively, lower in energy than the most stable structures found previously for the same number of hydrogen atoms[31] [M(2,2,2), D(4,2,2), and D(2,4,4)], see Table I.

It is convenient at this point to consider the adsorption energy E_a as a function of the hydrogen chemical potential,

TABLE I. Adsorption energy E_a^0, Eq. (2), for the most stable structures found in our calculations for the adsorption of 2–14 hydrogen atoms per 3×2 unit cell in the Si-rich 3C-SiC(100)-3×2 surface. Also shown are the values of E_a^0 for other structures such as D(3,0,0), B(2,1,2), M(2,2,2), D(3,2,2), D(4,2,2), D(3,4,2), and D(2,4,4), that have been previously obtained as lowest-energy structures (Refs. 31 and 33). N_H is the number of hydrogen atoms.

N_H	Structure	E_a^0 (eV)	N_H	Structure	E_a^0 (eV)
2	M(2,0,0)	−1.97	7	D(4,3,0)	−1.70
			7	D(3,2,2)	−0.74
3	B(2,0,1)	−1.50			
3	B(2,1,0)	−1.28	8	T(6,2,0)	−2.54
3	M(2,1,0)	−1.26	8	T(5,3,0)	−2.30
3	D(3,0,0)	−0.89	8	D(4,2,2)	−1.85
4	D(4,0,0)	−2.12	9	T(5,4,0)	−1.82
4	D(3,1,0)	−2.01	9	D(3,4,2)	−0.04
4	M(2,1,1)	−1.77			
4	B(2,0,2)	−0.71	10	T(4,5,1)	−2.62
			10	D(4,4,2)	−2.54
5	D(4,1,0)	−1.34	10	D(2,4,4)	−0.67
5	B(2,1,2)	−1.30			
			12	T(6,4,2)	−2.50
6	T(4,2,0)	−2.31	12	T(5,5,2)	−2.39
6	T(5,1,0)	−2.27			
6	D(4,2,0)	−2.26	14	T(5,6,3)	−2.66
6	M(2,2,2)	−1.87			

Eq. (1), for the most stable structures found in our work, see Fig. 3. In this figure the origin of the hydrogen chemical potential is taken at $\mu_H^0=\frac{1}{2}E[H_2]$, i.e., we plot $E_a(\Delta\mu_H)$, where $\Delta\mu_H=\mu_H-\mu_H^0$.

The plot of the adsorption energy as function of the hydrogen chemical potential reveals the stable structures when changing from hydrogen poor conditions to hydrogen rich conditions. For the lower values of the hydrogen chemical potential the most stable structure is the M(2,0,0), as expected and in agreement with previous findings.[31,33] In our calculations the M(2,0,0) structure is the most stable in the range $-0.99<\Delta\mu_H<-0.095$ eV (for $\Delta\mu_H<-0.99$ eV the clean surface is more stable). As μ_H increases, we find that the following stable structure is not D(4,0,0) (Refs. 31 and 33) but the T(6,2,0) structure, that contains eight hydrogen atoms in the 3×2 unit cell. The transition between M(2,0,0) and T(6,2,0) occurs at $\Delta\mu_H=-0.095$ eV. The T(6,2,0) structure is the most stable in the range $-0.095<\Delta\mu_H<-0.04$ eV; then, for a narrow range of chemical potential, $-0.04<\Delta\mu_H<-0.01$ eV, the most stable is a structure with ten hydrogen atoms, T(4,5,1). This structure involves breaking and rebonding of Si-Si bonds, see below. Finally, for $\Delta\mu_H>-0.01$ eV the most stable is the T(5,6,3) structure that contains 14 hydrogen atoms in the unit cell. Notice that all these transitions occur within a hydrogen chemical potential range of ~0.1 eV, below $\mu_H^0=\frac{1}{2}E[H_2]$. As mentioned above, μ_H^0 corresponds to the upper limit of the hydrogen chemical potential for a surface interacting with an atmosphere of H_2 molecules. The inset of Fig. 3 shows the GGA result for the M(2,0,0), D(4,0,0), and T(6,2,0) structures close to their crossing points.

The T(6,2,0) structure is shown in Fig. 4(a). In this structure all the Si atoms of the first layer are bonded to three hydrogen atoms, forming SiH_3 units. There are two SiH_3 units in the 3×2 unit cell; each of these SiH_3 groups is bonded to one Si atom of the second layer and the other two Si atoms of the second layer are saturated by a single hydrogen atom. The Si atoms of the second layer form two other bonds with third-layer Si atoms and a *dimer* bond with another second-layer Si atom.

Figure 4(b) shows the second most stable structure we have found for eight hydrogen atoms, T(5,3,0). In this structure a Si_2H_5 group is bonded to a second-layer Si atom and the three other Si atoms of the second layer are saturated with one hydrogen atom. Notice that this structure presents eight different degenerate structures since there are four possible adsorption sites in the 3×2 unit cell for the Si_2H_5 group and two different arrangements for the Si dimers of the second layer. Similarly, the T(6,2,0) structure also presents several degenerate structures associated with the different arrangements of the SiH_3 and SiH groups and the dimer bonds of the second layer. There is also a second group of quasidegenerate T(6,2,0) structures with total energy only 0.01 eV higher than the structure shown in Fig. 4(a); in these T(6,2,0) structures the SiH_3 groups are on the same row along the $\times3$ direction. Notice that all this degeneracy may easily induce structural disorder along the $\times2$ direction. This disorder along the $\times2$ direction is related to the rupture of Si-Si bonds between first- and second-layer Si atoms. The struc-

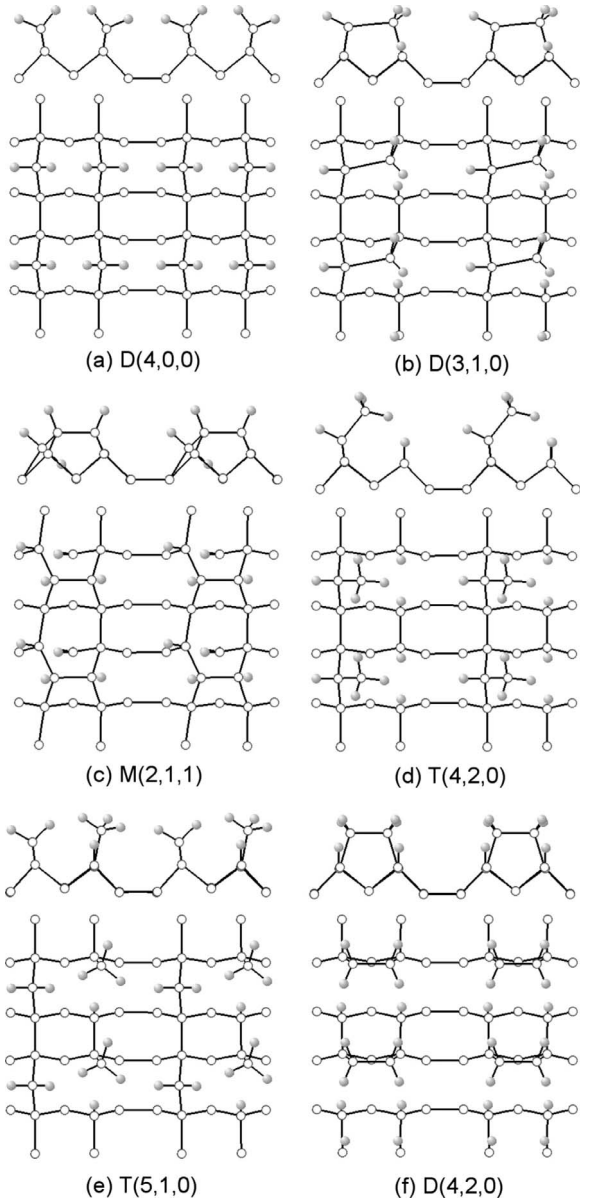

FIG. 2. Most stable atomic models for the adsorption of four [(a)–(c)] and six [(d)–(f)] hydrogen atoms in a SiC(100)-3×2 surface, see Table I.

tures shown in Fig. 4 could be a starting point for desorption of SiH_4 or Si_2H_6 molecules from the surface since they present SiH_3 or Si_2H_5 groups bonded to the surface by a single Si-Si bond. This will be discussed below.

Figure 5 show the most stable structures of Fig. 3, excepting the monohydride M(2,0,0) shown in Fig. 1. Figure 5(a) is the T(6,2,0), also shown in Fig. 4(a) discussed above. Figure 5(b) shows structure T(4,5,1), which in our calculations is the most stable structure in the range $-0.04 < \Delta\mu_H < -0.01$ eV. In this structure one Si atom of the first layer has broken its two original bonds with second-layer Si atoms, and has formed a new bond with a different second-layer Si atom. At this hydrogen coverage hydrogen atoms begin also to break Si-Si bonds between second- and third-layer Si atoms. Figure 5(c) shows a structure with 14 hydrogen atoms, T(5,6,3), which is the most stable in Fig. 3 for

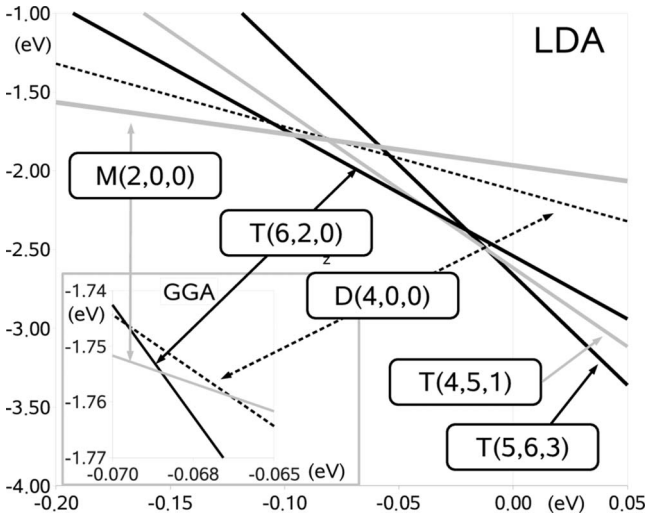

FIG. 3. Adsorption energy E_a, Eq. (1), as a function of the hydrogen chemical potential μ_H for the most stable H/SiC(100)-3×2 structures found in our work. μ_H is measured with respect to $\mu_H^0 = \frac{1}{2}E[H_2]$, i.e., $\Delta\mu_H = \mu_H - \mu_H^0$. The inset shows the GGA results close to the crossing point between M(2,0,0) and T(6,2,0) structures.

$\Delta\mu_H > -0.01$ eV. This structure presents two Si_2H_5 groups per 3×2 unit cell and also would present structural disorder along the ×2 direction due to existence of several degenerate structures, similar to the T(6,2,0) case discussed above [a similar structural disorder may be found in structures of the type of T(4,5,1), Fig. 5(b)]. Moreover, the rupture of Si-Si bonds between second- and third-layer Si atoms in Figs. 5(b) and 5(c) facilitates the appearance of structural disorder also along the ×3 direction, for example, in Fig. 5(c) the Si dimers in the third layer can appear at both sides of the Si_2H_5 group, with the corresponding rearrangement of the Si-H bonds in the third layer.

We discuss now the experimental evidence in comparison with our theoretical results. As mentioned above, the hydrogenated 3C-SiC(100)-3×2 surface has been prepared by exposing a clean 3×2 surface to atomic hydrogen dissociated by a hot tungsten filament. This results in an atmosphere of H_2 molecules with a ~5% of atomic H.[32] If the surface is at room temperature during hydrogen adsorption,[27] a 3×1

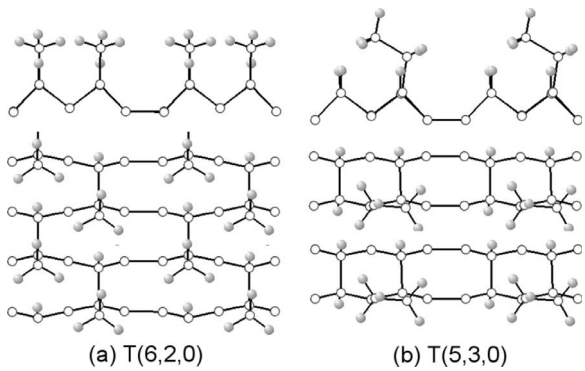

FIG. 4. Most stable atomic models for the adsorption of eight hydrogen atoms in a SiC(100)-3×2 surface

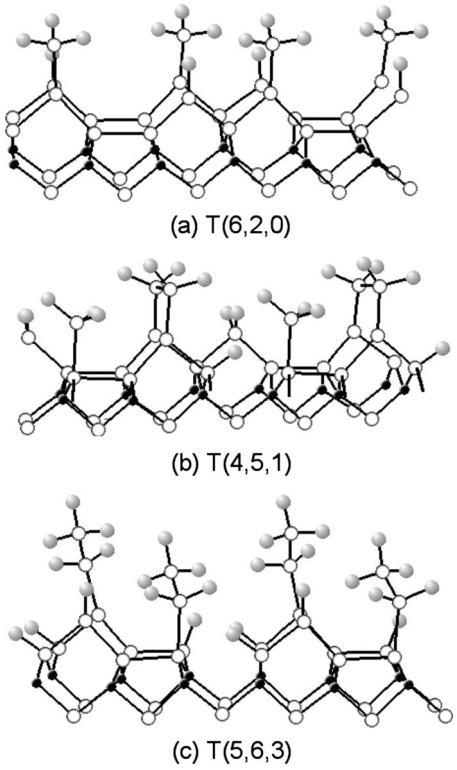

FIG. 5. Most stable atomic models for the adsorption of 8, 10, and 14 hydrogen atoms in a SiC(100)-3×2 surface. These are the stable structures as the hydrogen chemical potential is increased, after the monohydride M(2,0,0) surface shown in Figs. 1(b) and 1(c).

low-energy electron diffraction (LEED) pattern is observed for exposures of the order of 400–500 L (L=Langmuir). Photoemission experiments for this H/SiC(100)-3×1 surface show a hydrogen-induced surface resonance at ~4.6–4.9 eV below the valence-band maximum (VBM).[27] At higher hydrogen exposures the 3×1 order is destroyed and a 1×1 pattern is observed. On the other hand, if hydrogen exposures are performed at a temperature of 300 °C,[18,29,32] metallization of the surface is observed for H_2 exposures of ~20 L.[18]

Based on our calculations, the appearance of a 3×1 symmetry can be explained as due to the formation of the T(6,2,0) surface, Fig. 4(a). This is the first stable structure that appears after saturation of the Si dangling bonds of the first layer (Fig. 3); as mentioned above, the different degenerate and quasidegenerate structures for this T(6,2,0) surface easily induce structural disorder in the "×2" direction, yielding the observed 3×1 LEED pattern. The calculated density of states (DOS) for this surface also supports this interpretation. As shown in Fig. 6, the DOS for this surface presents a strong hydrogen-induced resonance ~5 eV below the VBM, in good agreement with experiment.[27] At higher hydrogen exposures, our results suggest that structures such as the T(4,5,1) and T(5,6,3) should appear. In this type of structures the rupture of Si-Si bonds between second- and third-layer Si atoms results in structural disorder along the ×3 direction, yielding the observed 1×1 LEED pattern. Thus, we find that in the SiC(100)-3×2 surface structural disorder along the

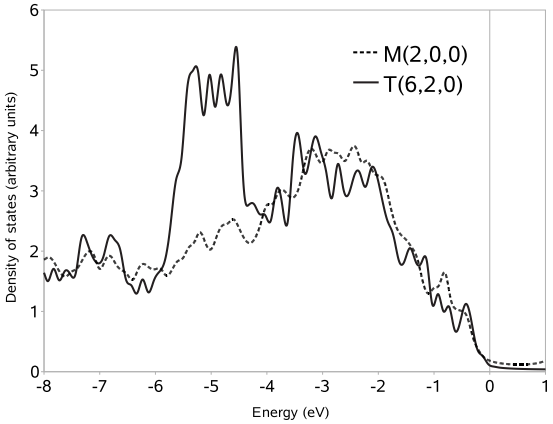

FIG. 6. Density of states for the M(2,0,0) and T(6,2,0) structures in the hydrogen atoms and three upper Si layers, calculated with the FIREBALL code.

×2 direction is due to the rupture of Si-Si bonds between first- and second-layer Si atoms while structural disorder along the ×3 direction is related to the rupture of Si-Si bonds between second- and third-layer Si atoms.

B. Hydrogen-induced metallization of SiC(100)-3×2

We discuss now the observed metallization. Initially, the metallization of the SiC(100)-3×2 upon interaction with hydrogen was explained in terms of a structural model with four hydrogen atoms per 3×2 unit cell, two saturating the dangling bonds of the first-layer dimer and the other two bonded to third-layer Si atoms, breaking the third-layer dimer bond, and leaving two Si dangling bonds in the third layer[18] [i.e., a M(2,0,2) model in our notation]. This structural model was inspired by infrared absorption spectroscopy (IRAS) experiments for the metallized surface that show two bands at 2118 and 2140 cm^{-1} (these bands are only observed in the *p*-polarized experiments, as corresponds to a metallic surface). The first one was assigned to Si-H bonds at the Si first layer while the second was assigned to Si-H bonds with the Si atom directly bonded to a C atom (i.e., third-layer Si atoms). This proposal was followed by several DFT calculations[33–36] that showed that this structure is not stable; instead, an alternative model was proposed in which the H atoms on the third layer occupy bridge positions on top of the third-layer Si dimer,[33–37] [i.e., a B(2,0,2) model in our notation]; some of these calculations, however, already noted that for this coverage the D(4,0,0) model was clearly more stable than the B(2,0,2) (Refs. 33 and 34) (see also Table I). Recently, an alternative explanation has been proposed based in DFT calculations of ~50 surface structures with 2–14 hydrogen atoms per 3×2 unit cell.[31] In these calculations, the structure D(4,0,0) is the most stable structure for a range of hydrogen chemical potential between the M(2,0,0) structure up to hydrogen concentrations where etching starts. The metallic behavior of the surface is explained in terms of band-bending effects before and after hydrogenation due to surface dangling bonds and the spontaneous polarization of SiC, respectively.[31]

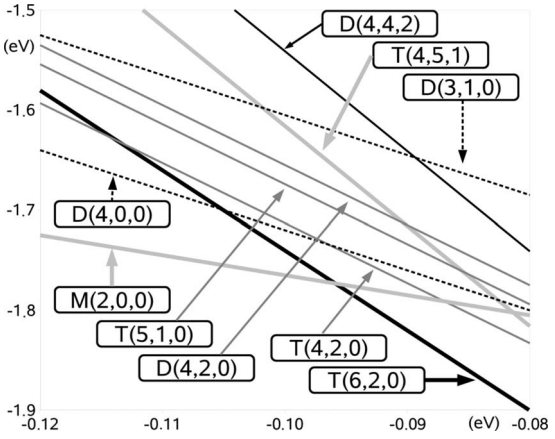

FIG. 7. Adsorption energy E_a, Eq. (1), as a function of the hydrogen chemical potential $\Delta\mu_H$ close to the transition between the M(2,0,0) and T(6,2,0) structures. Notice the different energy scales as compared with Fig. 3.

In our calculations we find that all the most stable structures as a function of the hydrogen chemical potential [M(2,0,0), T(6,2,0), T(4,5,1), and T(5,6,3)] are insulating, and therefore the observed metallization cannot be explained in terms of stable structures at $T=0$ K. This result suggests that this hydrogen-induced metallization should be related to dynamical effects. In particular, when the SiC(100)-3×2 surface is interacting with an atmosphere of atomic hydrogen at a temperature of $T=300$ C, there is a high probability[48] that an incoming hydrogen atom reacts with an already adsorbed hydrogen atom to form a H_2 molecule that desorbs from the surface, leaving behind a Si dangling bond. The dynamical equilibrium between this abstraction of H atoms and the adsorption of H atoms determines the structure of the surface at the different experimental conditions. For example, this abstraction of H atoms is the reason why H atoms do not saturate all the Si dangling bonds at the Si(100)-2×1 phase at $T=400$ °C.[48]

The experimental evidence suggests that the observed metallization occurs close to the transition between the M(2,0,0) and T(6,2,0) structures. For example, the IRAS spectrum for the metallic surface[18] shows a prominent peak associated with H atoms adsorbed on the top dimers and an extra small peak at 2140 cm^{-1}. Figure 7 shows an expanded image of Fig. 3 close to the transition between the M(2,0,0) and T(6,2,0) structures; in this figure we have included also other structures from Table I not shown in Fig. 3 for clarity. In order to transit from the M(2,0,0) to the T(6,2,0) structure, six extra hydrogen atoms per 3×2 unit cell must be adsorbed in the surface. Incoming hydrogen atoms have to start breaking Si-Si bonds: two hydrogen atoms are required to saturate the two Si dangling bonds that result from the rupture of a Si-Si bond. As shown in Fig. 7, close to the transition point between the M(2,0,0) and T(6,2,0) structures there are four competing lowest-energy structures whose adsorption energies E_a differ by only ~0.05 eV per 3×2 unit cell, the number of hydrogen atoms in these structures oscillating between 2 and 8 per 3×2 unit cell. Thus, a possible explanation for the observed metallization is that at $T=300$ °C the surface, in the presence of an atmosphere of atomic hydrogen, is locally fluctuating between these structures by means of the dynamical adsorption/desorption of hydrogen and rupture/formation of Si-Si bonds. These processes involve the dynamical formation of Si dangling bonds, explaining the observed metallization. As more hydrogen atoms are adsorbed on the surface and the transit to the T(6,2,0) structure is completed the surface becomes again insulating, in agreement with experiment.[49] In this case, the 2140 cm^{-1} peak observed in IRAS (Ref. 18) would be explained as resulting from the Si-H bonds present in SiH_3 groups, for example, in the Si(100) surface, peaks observed in IRAS in the range 2130 cm^{-1}–2150 cm^{-1} are associated with trihydride SiH_3 units.[50,51] The isotopic effect observed in the deuterium-induced metallization of SiC(100)-3×2 (Ref. 30) can also be explained in this scenario as resulting from the lower mobility of the deuterium atoms as compared to hydrogen atoms, and, e.g., the lower rate of desorbing D_2 (instead of H_2) molecules from the surface at the same temperature.

C. Desorption of SiH_4 molecules from the Si-rich SiC(100) surface

We briefly examine here the desorption of SiH_4 and Si_2H_6 molecules from the hydrogenated SiC(100)-3×2 surface. Notice in Figs. 4 and 5 already the presence of SiH_3 and Si_2H_5 groups that are bonded to the surface by one Si-Si bond. This suggest that further hydrogen atoms could replace this Si-Si bonds by two Si-H bonds, resulting in the desorption of SiH_4 and Si_2H_6 molecules from the surface. In order to gain some insight into this process we examine here the energetics of it as a function of the hydrogen chemical potential. For this purpose, we have analyzed diverse hydrogenated SiC(100)-3×2 surface structures in which a number N_D of SiH_4 molecules are removed from the surface and calculate the following energy:

$$E_D = E[\mathrm{H/SiC}] + N_D E[\mathrm{SiH_4}] - E_{\mathrm{SURF}}[3\times 2] - N_{\mathrm{H}}\mu_{\mathrm{H}}, \tag{3}$$

where $E[\mathrm{H/SiC}]$ is the energy of the remaining hydrogenated surface, $E[\mathrm{SiH_4}]$ is the energy of a SiH_4 molecule (including zero-point energy of the Si-H bonds[47]), $E[3\times 2]$ is the energy of the clean SiC(100)-3×2 surface, and N_H is the number of hydrogen atoms on the surface and on the SiH_4 molecules. We have considered N_D values from 1 to 6. The most sable cases we have found for each value of N_D are shown in Figs. 8(a)–8(f). Structures Figs. 8(a)–8(c) present SiH_3 and SiH groups and structures (d)–(f) contain SiH_2 and SiH groups. In the case of structure 8(f), the first two Si layers have been completely removed and thus it corresponds to a Si coverage $\theta=1$, with both monohydride and dihydride Si atoms, forming a 3×1 reconstruction similar to the Si(100)-3×1 surface.[47] Also shown in this figure are the monohydride surface for $\theta=1$ [Figs. 8(g) and 8(h)] and the monohydride and dihydride surfaces for Si coverage $\theta=1.5$ (Refs. 25 and 52) [Figs. 8(i) and 8(j)]. These last three structures have been calculated in a 4×2 surface unit cell.

The relative stability of these structures is explored in Fig. 9, where we plot E_D, Eq. (3), as a function of the hydrogen chemical potential; in this figure we have used as reference

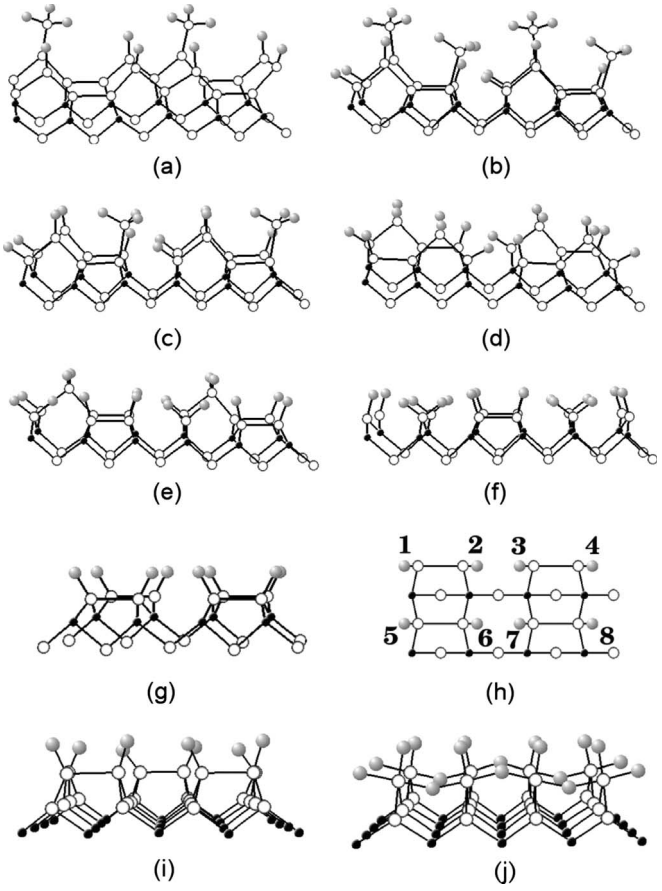

FIG. 8. [(a)–(f)] The most stable hydrogenated SiC(100)-3×2 surfaces for one to six SiH_4 molecules desorbed from the surface. [(g) and (h)] $\theta=1$ monohydride H/SiC(100)-2×1 surface; (h) top view. (i) monohydride and (j) dihydride structures for a Si coverage of $\theta=1.5$. Figures 8(i) and 8(j) are rotated 90° as compared to Figs. 8(a)–8(g).

the SiC(100)-3×2 surface hydrogenated with 14 hydrogen atoms, structure T(5,6,3), which is the most stable structure in Fig. 3 for $\Delta\mu_H > -0.01$ eV; the energies corresponding to structures (g)–(j) that have been calculated in a 4×2 unit cell are rescaled to correspond to a 3×2 unit cell. This figure shows that desorption of SiH_4 molecules is not energetically favored until positive values of $\Delta\mu_H$, i.e., $\mu_H > \mu_H^0$. This result is in agreement with the experimental observation that a good quality 3C-SiC(100)-3×2 clean surface is recovered from both the 3×1 and 1×1 hydrogenated surfaces by hydrogen desorption at 900–1000 °C.[27]

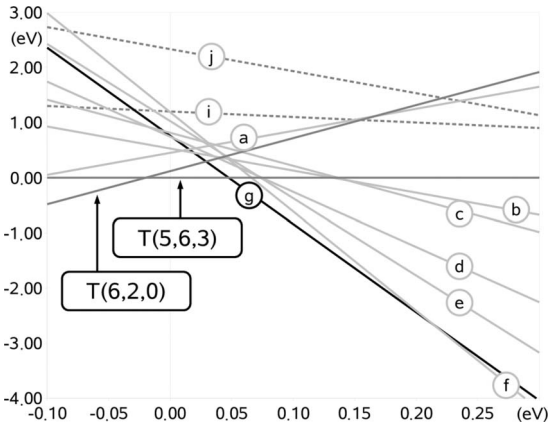

FIG. 9. Energy E_D, see Eq. (3), as a function of the hydrogen chemical potential for the hydrogenated SiC(100) surfaces shown in Fig. 8.

D. Hydrogenation of the Si-poor SiC(100) surface

In Fig. 9 the lowest-energy structures for increasing values of μ_H are the structures shown in Figs. 8(g) and 8(f). In these two structures the Si coverage above the last C layer is $\theta=1$; Fig. 8(f) presents a 3×1 symmetry and Fig. 8(g) a 2×1. An analysis of the adsorption energy E_a as a function of the hydrogen chemical potential (similar to that shown in Fig. 3) for the $\theta=1$ SiC(100) surface shows that the monohydride 2×1 surface, Fig. 8(g) is the most stable for a wide range of hydrogen chemical potentials, from $\Delta\mu_H=-1.23$ eV up to $\Delta\mu_H=+0.21$ eV. In this surface the Si atoms of the upper layer form strong dimer bonds, with a Si-Si distance of $d=2.36$ Å, and hydrogen atoms saturate the remaining dangling bonds (one per Si atom on the surface). Below $\Delta\mu_H=-1.37$ eV the clean $\theta=1$ SiC(100) surface is the most stable while the range $-1.37<\Delta\mu_H<-1.23$ eV corresponds to lower hydrogen coverages (i.e., one to seven hydrogen atoms in a 4×2 unit cell, see Table II), with hydrogen atoms attached to Si dangling bonds. Above $\Delta\mu_H=+0.21$ eV the 3×1 reconstruction, Fig. 8(f) is the most stable case.

We have also considered the hydrogenation of the 3C-SiC(100) surface with Si coverage $\theta=1.5$. Figure 8(i) shows the monohydride case and Fig. 8(j) the dihydride surface; these $\theta=1.5$ surfaces present $c(4\times2)$ and 2×1 symmetry, respectively. Our calculations yield adsorption energies, $E_a^0=-4.9$ eV and −3.4 eV per 4×2 unit cell, for the monohydride and dihydride $\theta=1.5$ surfaces, respectively. The monohydride $c(4\times2)$ surface is the stable $\theta=1.5$ structure in the hydrogen chemical potential range $-1.22<\Delta\mu_H<+0.38$ eV; below $\Delta\mu_H=-1.22$ eV the clean $\theta=1.5$ surface is the stable structure while the dihydride 2×1 surface would be the stable $\theta=1.5$ structure for $\mu_H>+0.38$ eV, i.e., above the upper limit for μ_H [notice that the 3C-SiC(100)$c(4\times2)$ surface can be hydrogenated in an atmosphere of H_2 molecules, without the presence of atomic hydrogen[40]].

Two main structural models have been discussed regarding the 3C-SiC(100)$c(4\times2)$ atomic structure, with two different Si coverages θ above the last C layer. In the alternatively up and down (AUDD) model,[24] the surface is terminated by a Si monolayer ($\theta=1$), the Si atoms forming alternatively up and down symmetric dimers while the missing row antisymmetric dimer (MRAD) model[25] consists of asymmetric Si dimers on top of a full Si ML ($\theta=1.5$). Although the experimental evidence seems to favor the AUDD model over the MRAD,[12] DFT calculations show the AUDD structure is not stable without artificially introducing a significant strain in the calculations.[13,25,53,54] Also, DFT calculations of the formation energy of these surfaces concluded that the MRAD structure has a lower formation energy than

TABLE II. Adsorption energies E_a^0, Eq. (2), for one to eight hydrogen atoms per 4×2 unit cell adsorbed on the Si-poor $\theta=1$ 3C-SiC(100) surface (Ref. 23). The different structures are indicated by the position of the hydrogen atoms as shown in Fig. 8(h). N_H is the number of hydrogen atoms per 4×2 unit cell.

N_H	Structure	E_a^0 (eV)	N_H	Structure	E_a^0 (eV)
1	(1)	−1.37	3	(1,5,4)	−4.09
2	(1,2)	−2.40	3	(1,5,6)	−3.71
2	(1,3)	−2.47	3	(1,5,7)	−3.77
2	(1,4)	−2.72	4	(1,4,5,8)	−5.45
2	(1,5)	−2.74	5	(1,3,4,5,8)	−6.51
2	(1,6)	−2.49	6	(1,2,3,4,5,8)	−7.85
2	(1,7)	−2.51	6	(1,2,4,5,6,8)	−7.62
2	(1,8)	−2.69	6	(1,3,4,5,6,8)	−7.58
3	(1,5,2)	−3.71	7	(1,2,3,4,5,6,8)	−8.97
3	(1,5,3)	−3.77	8	(1,2,3,4,5,6,7,8)	−10.36

the AUDD for all allowed values of the Si chemical potential.[13] Recently, the atomic structures of 3C-SiC(100) for these two Si coverages have been analyzed using DFT molecular-dynamics and PW methods, obtaining new lower-energy structures.[23] In the case of the $\theta=1$ surface, the lowest-energy structures, without introducing strain in the calculations, are a 4×1 and 4×2 reconstructions.[23] These surfaces are 60 meV per 1×1 unit cell lower in energy than the ideal 1×1 surface; for comparison, the 2×1 reconstruction is only a few meV lower in energy than the 1×1,[25,53,55,56] and the AUDD is slightly above the 2×1.[13] In the case of $\theta=1.5$ a atomic structure with 4×2 symmetry was found to present a total energy slightly below the $c(4\times2)$-MRAD structure.[23]

The hydrogenation of the 3C-SiC(100)-$c(4\times2)$ surface has been studied experimentally.[32,40,41] Upon hydrogenation, the surface symmetry changes to 2×1; desorption of hydrogen at elevated temperatures restores the original $c(4\times2)$ surface.[40,41] Photoemission experiments shows a hydrogen-induced resonance at ~2.4 eV below the VBM.[41] These experimental results can be easily explained assuming a Si coverage of $\theta=1$; in this case hydrogenation results in the monohydride $\theta=1$ surface shown in Fig. 8(g). This structure presents a 2×1 translational symmetry and our results show it is the stable hydrogenated $\theta=1$ structure for a wide range of hydrogen chemical potentials, up to $\Delta\mu_H=+0.21$ eV. Moreover, previous calculations[52] have shown that this structure presents a prominent hydrogen-induced peak in the DOS at ~2.6 eV below the VBM, in good agreement with the hydrogen-induced resonance observed in photoemission experiments.[41] On the other hand, an explanation of the 2×1 symmetry in terms of a Si coverage of $\theta=1.5$ would imply the formation of the dihydride $\theta=1.5$ surface shown in Fig. 8(j), breaking the Si dimers of the top layer. Our calculations show that this structure is not stable (with respect to monohydride $\theta=1.5$ surface) until very high values of the hydrogen chemical potential, $\Delta\mu_H>+0.38$ eV. Also, this structure does not explain[52] the hydrogen-induced resonance observed in photoemission experiments.

Finally, we have also analyzed the initial adsorption of hydrogen atoms on the $\theta=1$ SiC(100) surface,[23] by considering the adsorption of one to eight hydrogen atoms per 4×2 unit cell [the case of eight hydrogen atoms corresponds to the 2×1 case of Fig. 8(g)]. Table II shows the adsorption energies E_a^0, Eq. (2), we have obtained for the different cases, and Fig. 8(h) shows the different adsorption sites (1–8) for the hydrogen atoms in the 4×2 unit cell. We find that initially (e.g., $N_H=2,3$) the lowest energy corresponds to hydrogen atoms adsorbed in neighboring Si dimers, with the adsorption of two hydrogen atoms in the same dimer being the least favorable case. The lowest adsorption energy E_a^0 for each value of N_H decreases almost linearly with the number of hydrogen atoms up to the saturation of all the Si dangling bonds for $N_H=8$. In particular, from $N_H=1$ to 4 it changes by ~−1.37 eV per hydrogen atom adsorbed on the surface. For the $N_H=8$ case, i.e., the monohydride 2×1 surface, Fig. 8(g), the adsorption energy E_a^0 per H atom, E_a^0/N_H, is −1.295 eV; this value can be compared with the monohydride $\theta=1.5$ [Fig. 8(i)] and $\theta=2$ [Fig. 1(b)] cases: in these three cases hydrogen atoms saturate the dangling bonds of Si dimers on the surface. We obtain $E_a^0/N_H=-1.225$ eV ($\theta=1.5$) and $E_a^0/N_H=-0.985$ eV ($\theta=2$), i.e., the bond energy of the hydrogen atoms on the Si dimers is reduced as the Si coverage increases.

IV. CONCLUSIONS

In conclusion, we have analyzed the hydrogenation of the Si-terminated surfaces, 3C-SiC(100)-3×2 and 3C-SiC(100)-$c(4\times2)$ using a combination of DFT techniques. For the Si-rich 3C-SiC(100)-3×2 case, the hydrogen atoms initially attach to the semiconductor dangling bonds in the first Si layer. After dangling-bond saturation, hydrogen atoms break Si-Si bonds between Si atoms of the first and second layer, replacing them by Si-H bonds, up to a hydrogen adsorption of eight hydrogen atoms per 3×2 unit cell. This results in the stable structure T(6,2,0) of Figs. 4(a) and 5(a). In this structure the Si atoms of the first layer are bonded to three hydrogen atoms, forming SiH_3 groups; also, the structural disorder of this structure along the $\times2$ direction, which is associated with the rupture of Si-Si bonds between Si atoms of the first and second layers, explains the

observed 3×1 phase.[27] At higher hydrogen adsorptions structures of the type of T(4,5,1) and T(5,6,3), Figs. 5(b) and 5(c) appear. In these structures, the rupture of Si-Si bonds between second- and third-layer Si atoms results in structural disorder along the $\times3$ direction, yielding the observed 1×1 phase.[27] The analysis of the adsorption energy as a function of the hydrogen chemical potential, Eq. (1), shows that the stable structures from hydrogen-poor to hydrogen-rich conditions appear in the following order: clean 3×2 surface$\rightarrow$M(2,0,0)$\rightarrow$T(6,2,0)$\rightarrow$T(4,5,1)$\rightarrow$T(5,6,3), see Figs. 1 and 5. All these structures are semiconducting/insulating. After our exhaustive consideration of possible adsorption geometries, we conclude that the observed metallization cannot be explained by exploring static structures. For the values of the hydrogen chemical potential where the transition between the M(2,0,0) and T(6,2,0) structures takes place, i.e., when hydrogen atoms start to replace Si-Si bonds by Si-H bonds, we find that the four lowest-energy structures present values of the adsorption energy E_a that differ by only $\sim$0.05 eV per 3×2 unit cell. The number of hydrogen atoms in these structures oscillates between two and eight per 3×2 unit cell. The observed hydrogen-induced metallization is explained as being due to a dynamical equilibrium between adsorption and abstraction of hydrogen atoms, close to the transition between the M(2,0,0) and T(6,2,0) structures, when the surface is exposed to an atmosphere of atomic hydrogen at a temperature of $\sim$300 °C. We also find in our calculations that desorption of SiH_4 molecules from this surface is not energetically favorable until values of the hydrogen chemical potential $\mu_H > \frac{1}{2}E[H_2]$.

Regarding the hydrogenation of the Si-poor 3C-SiC(100)-$c(4\times2)$ surface, we have considered the two proposed Si coverages θ for this surface, namely, $\theta=1$ and $\theta=1.5$. Experimentally, hydrogenation of this surface yields a 2×1 symmetry. For $\theta=1$ the monohydride H/SiC(100)-2×1 surface of Figs. 8(g) and 8(h) is the most stable hydrogenated surface for a wide range of hydrogen chemical potentials $-1.23<(\mu_H-\frac{1}{2}E[H_2])<+0.21$ eV, up to values of μ_H above $\frac{1}{2}$ the energy of the H_2 molecule. For $\theta=1.5$, a 2×1 surface can be obtained for the dihydride case, see Fig. 8(j). Our calculations show that this structure is only stable [as compared with the $\theta=1.5$ monohydride case of Fig. 8(i), that presents a $c(4\times2)$ symmetry] for $(\mu_H-\frac{1}{2}E[H_2])>+0.38$ eV. By comparing with the experimental evidence we conclude that the hydrogenated Si-poor H/SiC(100)-2×1 surface corresponds to a coverage of one Si monolayer above the last C layer, $\theta=1$.

ACKNOWLEDGMENTS

This work ws supported by Spanish MEyC under Contract Nos. MAT2007-60966 and MAT2008-02929-NAN. We thank Patrick Soukiassian and Enrique G. Michel for insightful discussions. We have used the free software xeo (project management for nanostructures, http://sourceforge.net/projects/xeo/) to handle the information of the many structures analyzed in this work.

[1] A. J. Mayne, D. Riedel, G. Comtet, and G. Dujardin, Prog. Surf. Sci. **81**, 1 (2006).
[2] J. J. Boland, Adv. Phys. **42**, 129 (1993).
[3] M. Dürr and U. Höfer, Surf. Sci. Rep. **61**, 465 (2006).
[4] K. Oura, V. G. Lifshits, A. A. Saranin, A. V. Zotov, and M. Katayama, Surf. Sci. Rep. **35**, 1 (1999).
[5] T. Seyller, J. Phys.: Condens. Matter **16**, S1755 (2004).
[6] A. R. Khan, A. Takeo, S. Ueno, S. Inanaga, T. Yamauchi, Y. Narita, H. Tsurumaki, and A. Namiki, Surf. Sci. **601**, 1635 (2007).
[7] Y. Narita, Y. Kihara, S. Inanaga, and A. Namiki, Surf. Sci. **603**, 1168 (2009).
[8] X.-Y. Peng, P. Krüger, and J. Pollmann, New J. Phys. **10**, 125028 (2008).
[9] A. Saedi, B. Poelsema, and H. J. W. Zandvliet, Phys. Rev. B **79**, 153402 (2009).
[10] W. Brenig and E. Pehike, Prog. Surf. Sci. **83**, 263 (2008).
[11] V. Y. Aristov, Phys. Usp. **44**, 761 (2001).
[12] P. Soukiassian and H. B. Enriquez, J. Phys.: Condens. Matter **16**, S1611 (2004).
[13] J. Pollmann and P. Krüger, J. Phys.: Condens. Matter **16**, S1659 (2004).
[14] V. Yu. Aristov, L. Douillard, O. Fauchoux, and P. Soukiassian, Phys. Rev. Lett. **79**, 3700 (1997).
[15] V. Ramachandran and R. M. Feenstra, Phys. Rev. Lett. **82**, 1000 (1999).
[16] F. Bechstedt and J. Furthmüller, J. Phys.: Condens. Matter **16**, S1721 (2004).
[17] P. Soukiassian, F. Semond, A. Mayne, and G. Dujardin, Phys. Rev. Lett. **79**, 2498 (1997).
[18] V. Derycke, Patrick G. Soukiassian, Fabrice Amy, Yves J. Chabal, Marie D. D'angelo, Hanna B. Enriquez, and Mathieu G. Silly, Nature Mater. **2**, 253 (2003).
[19] F. Amy, J. Phys. D **40**, 6201 (2007).
[20] S. Kim, J. Ihm, H. J. Choi, and Y.-W. Son, Phys. Rev. Lett. **100**, 176802 (2008).
[21] T. Ohta, Farid El Gabaly, Aaron Bostwick, Jessica L. McChesney, Konstantin V. Emtsev, Andreas K. Schmid, Thomas Seyller, Karsten Horn, and Eli Rotenberg, New J. Phys. **10**, 023034 (2008).
[22] A. Tejeda, D. Dunham, F. J. García de Abajo, J. D. Denlinger, E. Rotenberg, E. G. Michel, and P. Soukiassian, Phys. Rev. B **70**, 045317 (2004).
[23] D. G. Trabada and J. Ortega, J. Phys.: Condens. Matter **21**, 182003 (2009).
[24] P. Soukiassian, F. Semond, L. Douillard, A. Mayne, G. Dujardin, L. Pizzagalli, and C. Joachim, Phys. Rev. Lett. **78**, 907 (1997).
[25] W. Lu, P. Krüger, and J. P. Pollmann, Phys. Rev. Lett. **81**, 2292 (1998).
[26] P. Krüger and J. Pollmann, Phys. Rev. B **73**, 035327 (2006).
[27] H. W. Yeom, I. Matsuda, Y.-C. Chao, S. Hara, S. Yoshida, and R. I. G. Uhrberg, Phys. Rev. B **61**, R2417 (2000).

[28] M. G. Silly, C. Radtke, H. Enriquez, P. Soukiassian, S. Gardonio, P. Moras, and P. Perfetti Appl. Phys. Lett. **85**, 4893 (2004).
[29] M. D'angelo, H. Enriquez, N. Rodriguez, V. Yu. Aristov, P. Soukiassian, A. Tejeda, E. G. Michel, M. Pedio, C. Ottaviani, and P. Perfetti, J. Chem. Phys. **127**, 164716 (2007).
[30] J. Roy, V. Yu. Aristov, C. Radtke, P. Jaffrennou, H. Enriquez, P. Soukiassian, P. Moras, C. Spezzani, C. Crotti, and P. Perfetti, Appl. Phys. Lett. **89**, 042114 (2006).
[31] P. Deak, B. Aradi, J. M. Knaup, and T. Frauenheim, Phys. Rev. B **79**, 085314 (2009).
[32] F. Amy and Y. J. Chabal, J. Chem. Phys. **119**, 6201 (2003).
[33] X. Peng, P. Krüger, and J. Pollmann, Phys. Rev. B **72**, 245320 (2005).
[34] R. Di Felice, C. M. Bertoni, C. A. Pignedoli, and A. Catellani, Phys. Rev. Lett. **94**, 116103 (2005).
[35] H. Chang, J. Wu, B.-L. Gu, F. Liu, and W. Duan, Phys. Rev. Lett. **95**, 196803 (2005).
[36] F. B. Mota, V. B. Nascimento, and C. M. C. de Castilho, J. Phys.: Condens. Matter **17**, 4739 (2005).
[37] R. Rurali, E. Wachowitz, P. Hyldgaard, and P. Ordejón, Phys. Status Solidi (RRL) **2**, 218 (2008).
[38] X. Peng, P. Krüger, and J. Pollmann, Phys. Rev. B **75**, 073409 (2007).
[39] X. Peng, P. Krüger, and J. Pollmann, Phys. Rev. B **76**, 125303 (2007).
[40] V. Derycke, P. Fonteneau, N. P. Pham, and P. Soukiassian, Phys. Rev. B **63**, 201305(R) (2001).
[41] S. M. Widstrand, L. S. O. Johansson, K. O. Magnusson, M. I. Larsson, H. W. Yeom, S. Hara, and S. Yochida, Surf. Sci. **479**, 247 (2001).
[42] P. Jelinek, H. Wang, J. P. Lewis, O. F. Sankey, and J. Ortega, Phys. Rev. B **71**, 235101 (2005); J. P. Lewis, K. R. Glaesemann, G. A. Voth, J. Fritsch, A. A. Demkov, J. Ortega, and O. F. Sankey, *ibid.* **64**, 195103 (2001); A. A. Demkov, J. Ortega, O. F. Sankey, and M. P. Grumbach, *ibid.* **52**, 1618 (1995); O. F. Sankey and D. J. Niklewski, *ibid.* **40**, 3979 (1989).
[43] M. D. Segall, Philip J. D. Lindan, M. J. Probert, C. J. Pickard, P. J. Hasnip, S. J. Clark, and M. C. Payne, J. Phys.: Condens. Matter **14**, 2717 (2002).
[44] M. A. Basanta, Y. J. Dappe, P. Jelínek and J. Ortega, Comput. Mater. Sci. **39**, 759 (2007).
[45] W. Kohn and L. J. Sham, Phys. Rev. **140**, A1133 (1965).
[46] J. P. Perdew, K. Burke, and M. Ernzerhof, Phys. Rev. Lett. **77**, 3865 (1996).
[47] J. E. Northrup, Phys. Rev. B **44**, 1419 (1991).
[48] J. Dabrowski and H. J. Mussig, *Silicon Surfaces and the Formation of Interfaces* (World Scientific, Singapore, 2000), p. 275.
[49] P. Soukiassian (private communication).
[50] M. Niwano, M. Shinohara, Y. Neo, and K. Yokoo, Appl. Surf. Sci. **162-163**, 111 (2000).
[51] Y. Tsukidate and M. Suemitsu, Jpn. J. Appl. Phys., Part I **40**, 5206 (2001).
[52] X. Peng, Ling Ye, and Xun Wang, Surf. Sci. **571**, 21 (2004).
[53] A. Catellani, G. Galli, F. Gygi, and F. Pellacini, Phys. Rev. B **57**, 12255 (1998).
[54] A. Tejeda, E. Wimmer, P. Soukiassian, D. Dunham, E. Rotenberg, J. D. Denlinger, and E. G. Michel, Phys. Rev. B **75**, 195315 (2007).
[55] M. Sabisch, P. Krüger, A. Mazur, M. Rohlfing, and J. Pollmann, Phys. Rev. B **53**, 13121 (1996).
[56] P. Kackell, F. Bechstedt, H. Hüsken, B. Schröter, and W. Richter, Surf. Sci. **391**, L1183 (1997).